Electronic Supplementary Material (ESI) for Journal of Materials Chemistry B.

Supporting Information

Effective Co-delivery of Nutlin-3a and p53 genes via Core-shell Microparticles for Disruption of MDM2-p53 Interaction and Reactivation of p53 in Hepatocellular Carcinoma

*Pooya Davoodi [a], Madapusi P. Srinivasan [a,b] and Chi-Hwa Wang[*a]*

[a.] *Department of Chemical and Biomolecular Engineering, National University of Singapore, 4 Engineering Drive 4, Singapore 117585.*

[b.] *Civil, Environmental and Chemical Engineering, RMIT University, GPO Box 2476, Melbourne VIC 3001 Australia.*

**Corresponding author: Tel.: +65-65165079; Fax: +65-67791936, E-mail address: chewch@nus.edu.sg*

Table S1. Characterization of β-CD-g-CS: degree of substitution

Sample	β-CD:CS	Degree of substitution (%)
β-CD-g-CS (1:1)	0.87	4.31
β-CD-g-CS (2:1)	2.01	6.48
β-CD-g-CS (3:1)	3.02	6.99
β-CD-g-CS (6:1)	5.95	8.28

Table S2. Drug loading content (DLC) and encapsulation efficiency (EE) of nutlin-3a and p53-pDNA NPs loaded microparticles.

	Core compartment		Shell compartment*
	DLC	EE	EE
MPs1	3.36±0.29	83.95±7.25	-
MPs2	-	-	51.64±6.39
MPs3	2.77±0.23	69.22±5.81	49.21±4.94

* Theoretical loading: 150 μg of pDNA.

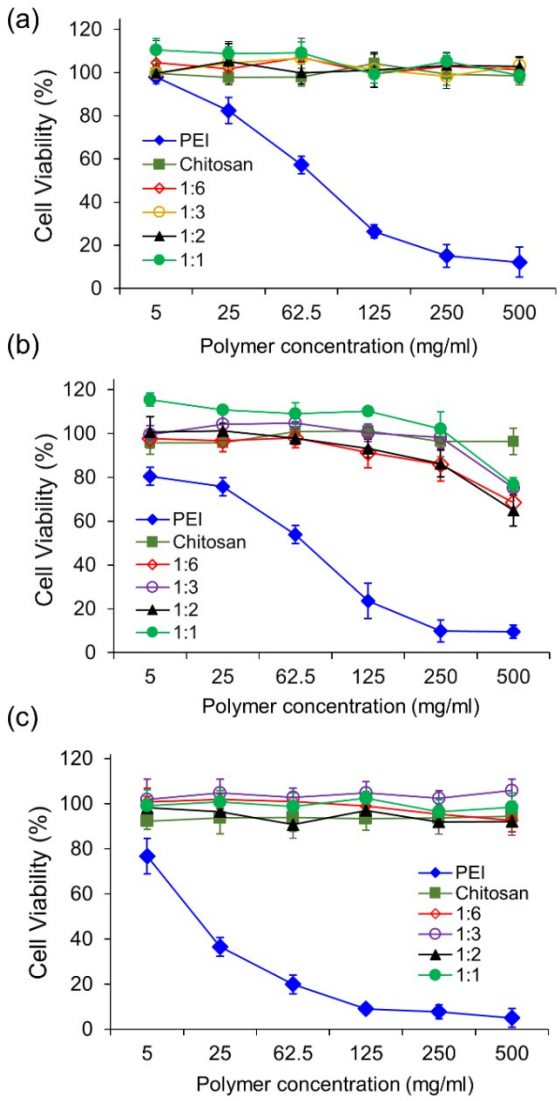

Figure S1. Cell viability of *β*-CD-g-CSs at different *β*-CD:CS ratios in (a) HepG2 (liver), (b) Hela (ovarian), and (c) C6 glioma (brain) cell lines. PEI-25k and pure CS were considered as controls. The cell viability was determined using MTS assay. Data represent mean ± standard deviation of at least n = 4.

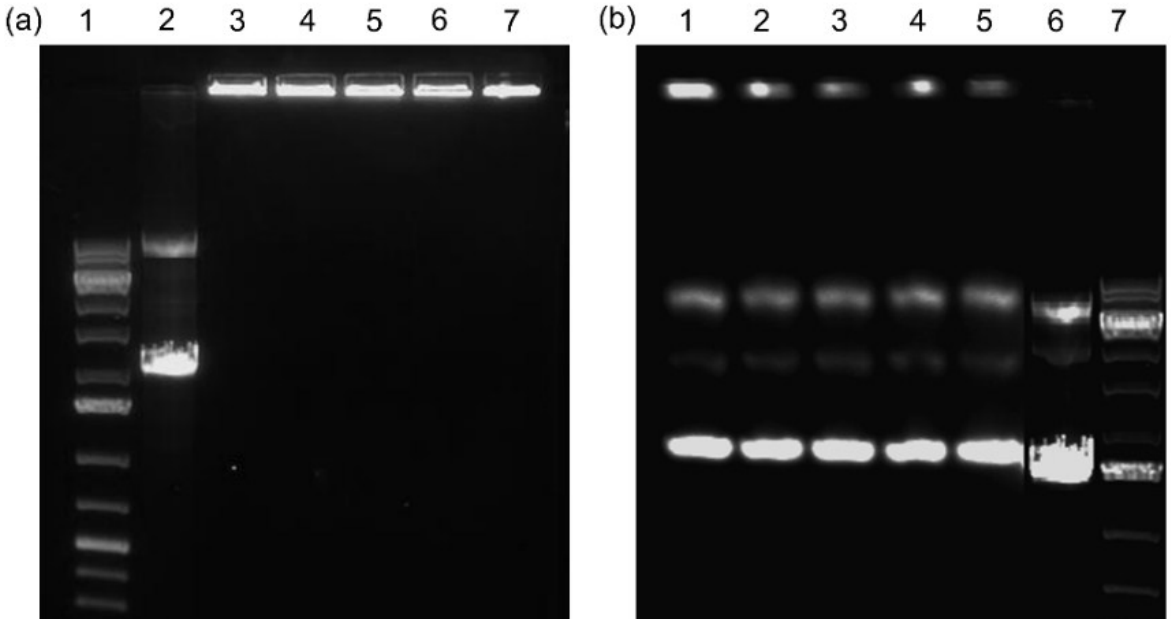

Figure S2. Gel retardation assay of pDNA/*β*-CD-g-CS NPs (*β*-CD:CS 3:1). (a) The binding efficiency of *β*-CD-g-CS with pDNA. Lane 1 contains 1 kb DNA ladder. Lane 2 contains 1.0 μg of naked DNA. Lanes 3 to 7 contained pDNA-NPs (2.0 μg) at N/P ratios of 4, 5, 6, 7, and 8, respectively. (b) The effect of *β*-CD-g-CS on integrity of pDNA by digesting the nanoparticles with 20 μl lysozyme (100 U/ml) and 80 μl chitosanase (0.25 U/ml) in 50 mM of acetate buffer (pH=5.5). Lane 1 to 5 contained pDNA-NPs (2.0 μg) at N/P ratios of 4, 5, 6, 7 and 8, respectively. Lane 6 contains 1.0 μg of naked DNA. Lane 7 contains 1 kb DNA ladder. All samples were electrophorezed in 1×TAE on a 1% agarose gel, stained with 1× SYBR® Gold Nucleic Acid Gel Stain solution, and visualized under an ultraviolet transilluminator and imaged using gel-doc system (G: BOX, Syngene).

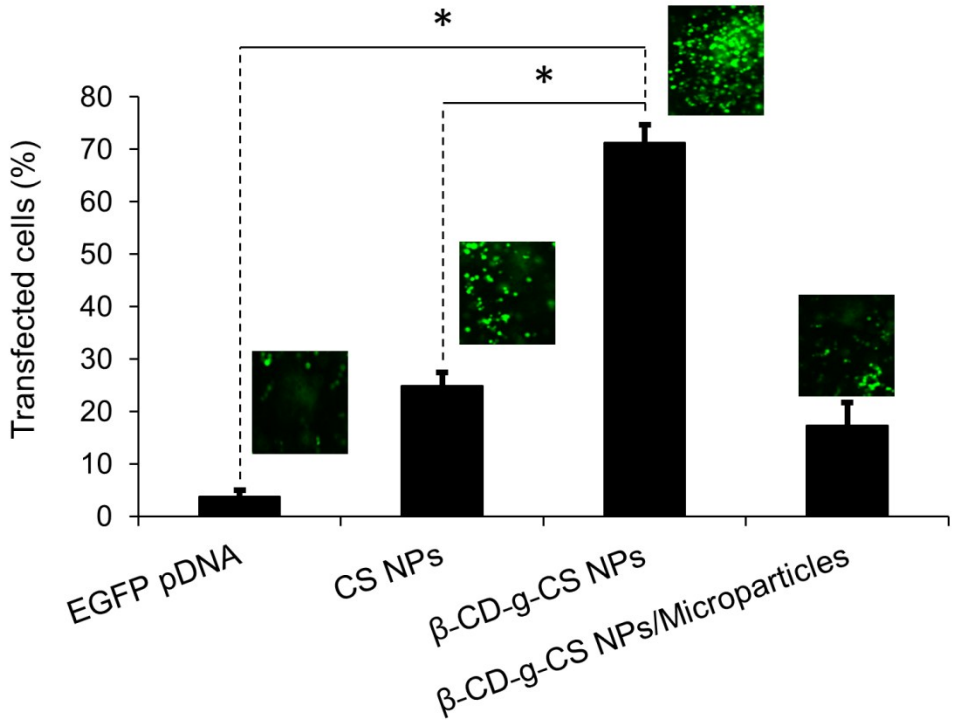

Figure S3. Measurement of cell transfection efficiency. Cells were treated by EGFP plasmid DNA, EGFP-pDNA-CS NPs, EGFP-pDNA-*β*-CD-g-CS NPs, and EGFP-pDNA-*β*-CD-g-CS NPs/microparticles encapsulated nanoparticles for 6 h. For microparticle formulation, the cells were incubated with particles for 2 days. Data represent mean ± standard deviation of n = 3.

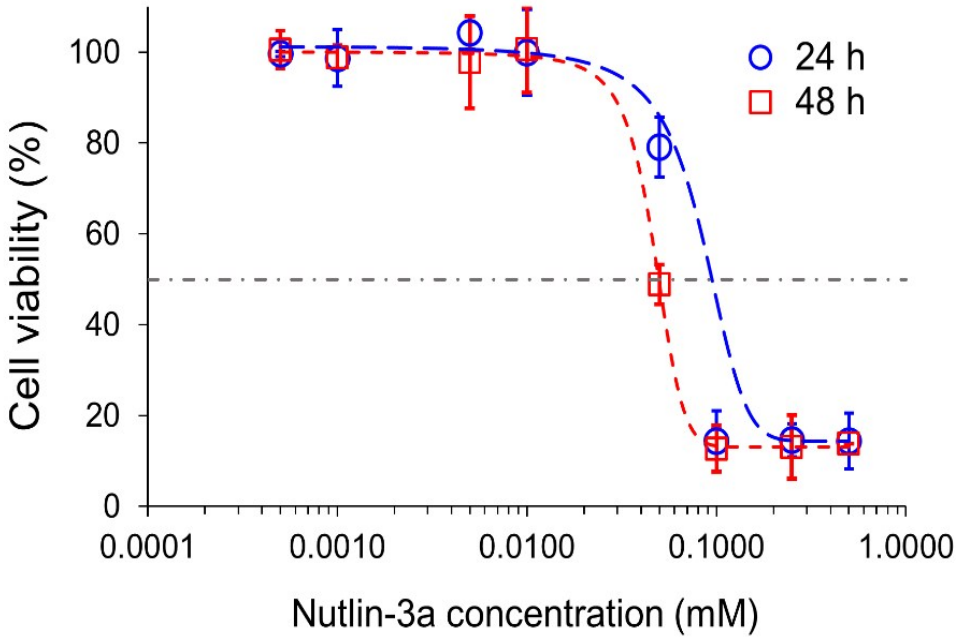

Figure S4. Cell viability results at different concentrations of nutlin-3a, where HepG2 cells were treated for 24 h and 48 h. Data represent mean ± standard deviation of n=4.

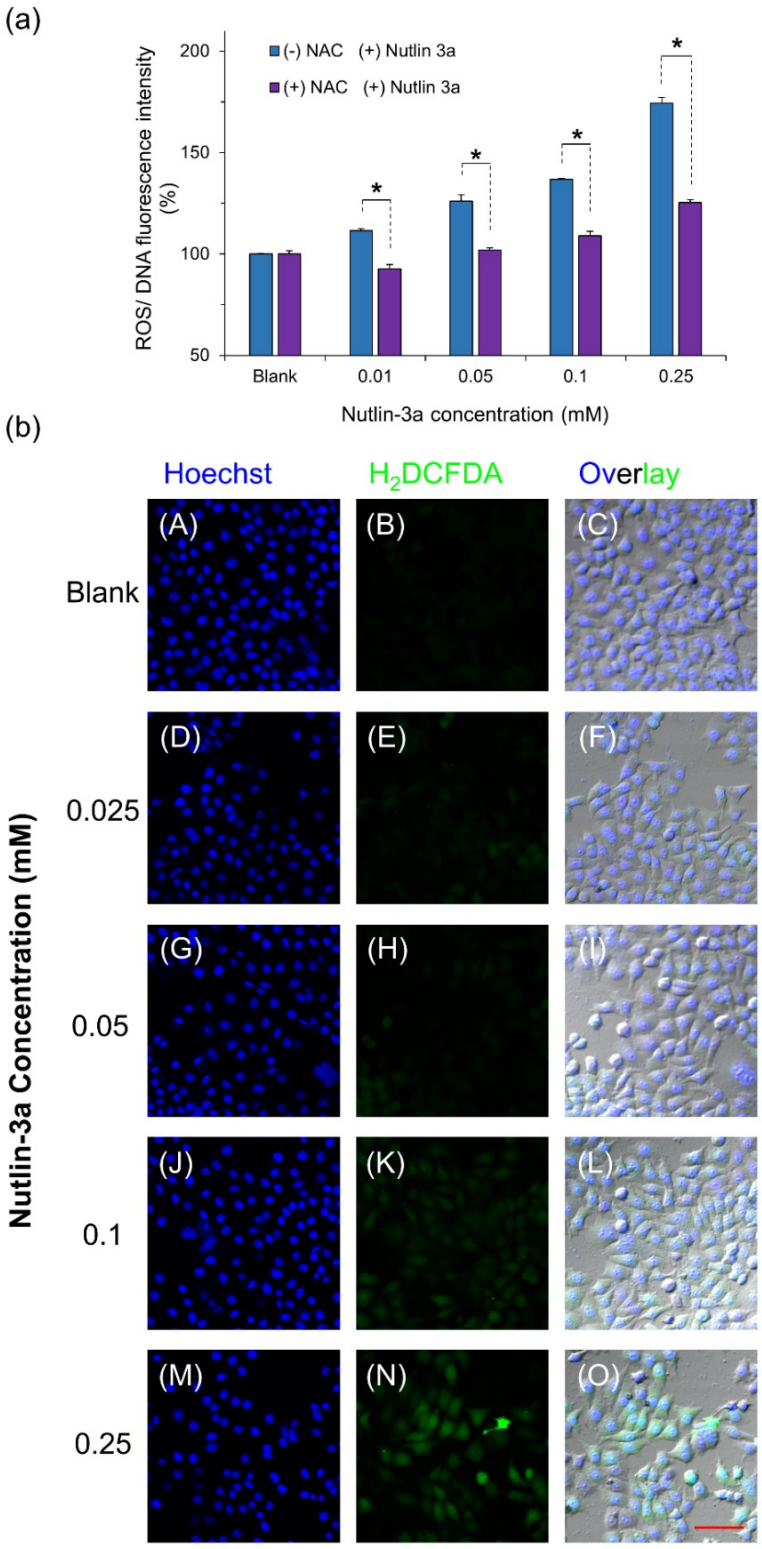

Figure S5. (a) Induction of intracellular ROS in non-apoptotic HepG2 cells. Temporal measurement of ROS levels following free-drugs exposure in HepG2 cells. The cells were

exposed to serially diluted nutlin-3a in the presence and absence of N-Acetyl-L-cysteine (NAC, ROS scavenger, Sigma-Aldrich). The ROS levels were measured after 4 h using H_2DCFDA fluorescent probes. ROS level of non-treated cells at each time-point was considered as negative control. (b) Confocal images depict the increase of intracellular ROS after 4 h of exposure to nutlin-3a solutions. Cell were stained with H_2DCFDA (ROS fluorescent probe: green light) and cell-permeant nuclear counterstain (Hoechst 33342: blue light). Data represent mean ± standard deviation of n=4. Statistical significance: * p <0.05. Scale bar= 25 μm.